Journal of Advanced Research in Applied Sciences and Engineering Technology

Journal homepage:
https://semarakilmu.com.my/journals/index.php/applied_sciences_eng_tech/index
ISSN: 2462-1943

An Evaluation of Fuzzy in Image Enhancement: Design and Comparison for Penicillium and Aspergillus Species

Farah Nabilah Zabani[1], Haryati Jaafar[1,*], Nur Rodiatul Raudah Mohamed Radzuan[1], Fatin Norazima Mohamad Ariff[1], Azirah Baharum[1]

[1] Department of Mechatronic Engineering, Faculty of Electrical Engineering and Technology, Universiti Malaysia Perlis, 02600 Arau, Perlis, Malaysia

ARTICLE INFO

Article history:
Received 17 August 2023
Received in revised form 19 September 2023
Accepted 11 April 2024
Available online 5 May 2024

Keywords:

Fuzzy-partition gamma adaptive histogram equalization (FpGAHE); Surrounding neighbourhood; Nearest neighbour; Image enhancement; Image classification

ABSTRACT

The main focus in this study is to enhance and classify the image of a type of filamentous fungi named Penicillium and Aspergillus. For image enhancement, fuzzy-partition gamma adaptive histogram equalization (FpGAHE) is proposed to improve the quality of an image, in particular the low quality of a microscopic image. Two stages have been considered in this technique. In the first stage, a fuzzy partition is developed to handle the inconsistency of the grey level values of the images by introducing a fuzzy set. In the second stage, surrounding neighbourhood is employed to avoid the imbalance data and reduce the drastically changes of brightness values of the image. The performances are evaluated into two parts i.e., image processing and image classification by using the collected microscopic images of fungi species. To evaluate the effectiveness of the proposed technique, the existing techniques, HE, AHE, CLAHE, GC and AGC is compared to the FpGAHE. In image processing, the result attained shows that the proposed technique has a better performance by obtaining the highest value for the PSNR, SSIM and FSIM evaluation for the species of A. terreus in clean condition. Meanwhile, in image classification, five different nearest neighbour classifiers have been tested. The results show the proposed FpGAHE with Improved Fuzzy-Based k Nearest Centroid Neighbour (IFkNCN) classifier perform the best result compared to other nearest neighbour classifier by obtaining the value of 92.59 and 93.95 for the salt and pepper and Gaussian noise corrupted images respectively.

1. Introduction

Penicillium and *Aspergillus* species are categorized as a type of filamentous fungi. Both fungi can be often found in either soil, decaying organic matter or seeds, where they live as saprophytes. These types of fungi can be in different kind of environments throughout the world. This is due to their growth which is largely determined by the availability of water [1]. Although these species have several advantages in food industry as preservative and flavouring agent, they have various

* *Corresponding author.*
E-mail address: haryati@unimap.edu.my

https://doi.org/10.37934/araset.44.2.5271

disadvantages that include food spoilage as well as human and animal infections. Some species produce dangerous mycotoxins that could cause serious health issues and even death.

Generally, identification of the *Penicillium* and *Aspergillus* species is depended largely on their macroscopic features (colony diameter, colour, texture, exudates, and colony texture) and microscopic features (conidia, phialide, metula and hyphae) [2-3]. Meanwhile, the arrangements of conidiophores help in the identification of filamentous fungi. Plus, the process in which spores are produced (conidial ontogeny) also helps in the identification. The method of slide culturing is the best method in preserving the actual structure of a fungus. It is also the method used to examine dermatophytes microscopically when the culture had form conidia or spores [4]. This method is cost effective, offers fast availability of results and the equipment are easily accessible [5]. However, the flaw is that this method has a low diagnosis accuracy and the time consumption is high. Plus, only an experienced microscopist can perform this method. Currently, there is no latest method that could resolve these issues [6]. Handling the diagnosis manually may lead to a false result which can cause many other problems.

Therefore, an image-analysis scheme has been proposed to automatically detect a fungal species based on its microscopic images. A number of automated fungi detection have been recently developed based on an image processing scheme. From the various types of microscopic image enhancement techniques, histogram equalization (HE) is one of the most basic procedures for the contrast enhancement of fungi images [7]. The technique increases the apparent contrast in the image by flattening the histogram of the number of image pixels at each grey level value [8]. The adaptive histogram equalization (AHE) was then introduced. It is a technique used to reduce the appearance of noise in the image while maintaining the brightness of some areas [9]. Next, clip limit adaptive histogram equalization (CLAHE) is developed. This technique is applied on the modified membership plane which is then remapped to the grey level intensity [10]. However, both of AHE and CLAHE have tendency to over-amplify noise in relatively homogeneous regions of an image which is not suitable to be applied for microscopic images. Due to the microscopic images being captured in low quality, they are prone to be exposed to different levels of noises and blurring due to the variations in illumination, background, and focus. Moreover, these techniques normally change the brightness of the image significantly. Thus, causing the output image to become saturated with very bright or dark intensity values [11].

Various techniques have been studied in the past to address the issue of undesired over-enhancement and noise amplification in image enhancement. One such technique that has garnered significant interest is the fuzzy logic system, as it has shown promising results. For instance, a novel approach to image segmentation using a combination of Dynamic Particle Swarm Optimization (DPSO) and the Fuzzy C-Means (FCM) algorithm has been proposed by Dhanachandra and Chanu, [12] to reduce image noise. This technique holds potential for effectively enhancing image quality while simultaneously minimizing noise and other unwanted artefacts. The problem of distinguishing edges of objects that are difficult to discern due to image vagueness was addressed by investigating a fuzzy edge detector by Versaci and Morabito, [13]. This detector is based on both fuzzy divergence, which is considered a distance, and fuzzy entropy minimization for the thresholding sub-step in grey-scale images. By incorporating these techniques, the detector aims to reduce the impact of vagueness in images, thereby improving the clarity of object edges. Overall, this approach holds potential for enhancing the accuracy and effectiveness of edge detection in situations where images may be characterized by inherent fuzziness.

This paper proposes a new approach to managing the low-quality of fungi images by utilizing the effectiveness of fuzzy logic in image processing. Specifically, the proposed approach is called fuzzy-partition gamma adaptive histogram equalization (FpGAHE), which is designed to overcome the

challenges of unwanted over-enhancement and noise amplification. By leveraging fuzzy logic techniques, FpGAHE does not only preserve image brightness but also improves the local contrast of the original image. This technique consists of two stages. First, fuzzy partition is computed based on fuzzy set theory to handle the inconsistency of grey level values in better way compared to classical AHE. In the second stage, SN is introduced to avoid the imbalance data in each partition to reduce the drastically changes of brightness values that causes degradation of the image.

The organizational arrangement of this paper is outlined as follows. Section 2 presents and described the proposed method. Subsequently, Section 3 displays the experimental result of the proposed method and its comparison with the other existing methods. Lastly, Section 4 concludes this paper.

2. Methodology

The overall architecture for this paper is illustrated as in Figure 1.

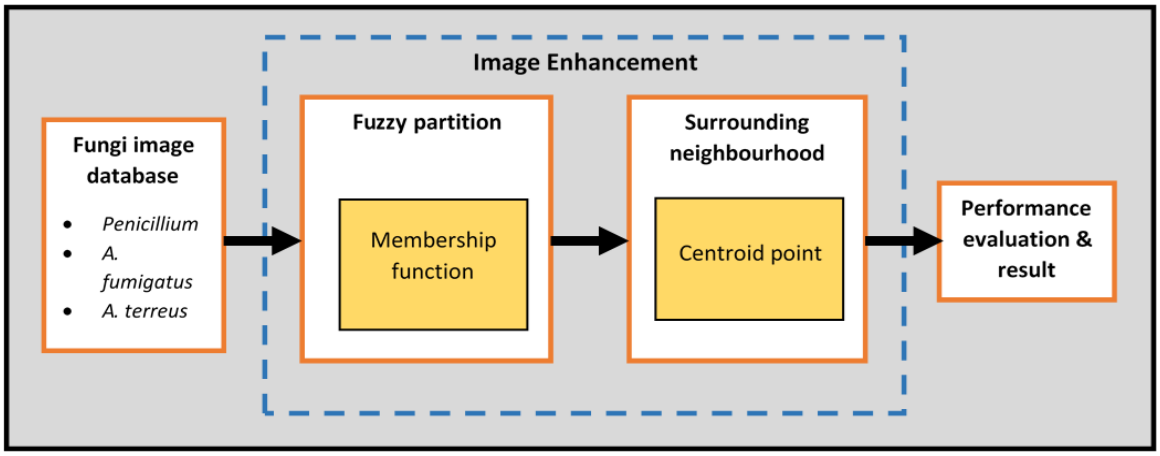

Fig. 1. Overall architecture of proposed method

2.1 Data Acquisition

The data is acquired from two different species of fungi, *Penicillium* and *Aspergillus* (*A. fumigatus* and *A. terreus*). Both of these fungi originate from the same family of fungi under the name of Trichocomaceae. The fungi image data were acquired from the Microbiology and Parasitology laboratory of Hospital Universiti Sains Malaysia located in Kubang Kerian, Kelantan. The process of data collection is done with permission from the hospital and the person in charge of the laboratory.

The microscopic examination was done by placing the glass slide under a microscope with a magnification of 40x. The image of fungi as seen under the microscope is displayed on the screen of a PC. Then, the preferred structure of fungi is captured by using Optikam B3 digital camera. A type of software, Optika Vision Lite, were used together with the Olympus CX31 microscope throughout this process. A sum of 194 coloured images with a resolution of 2048 x 1536 megapixels was captured. The images were saved in the form of JPG format. The fungi are differentiate based on their characteristics. To be able to do this, only the images of a fully matured fungi as shown in Table 1 are captured. From Table 1, the structure of each species can be seen clearly, and its microscopic characteristics can be easily identified. However, even though the structure of each species differs from one another, it could be confusing to identify each species if a large amount of it is needed to be identify.

Table 1
Examples of *Penicillium* and *Aspergillus sp.*

Scientific name and image		
Penicillium	A. terreus	A. fumigatus
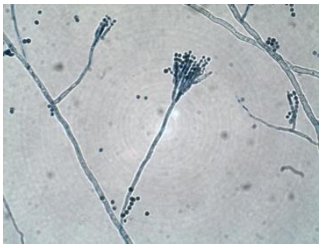	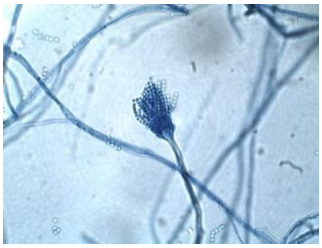	
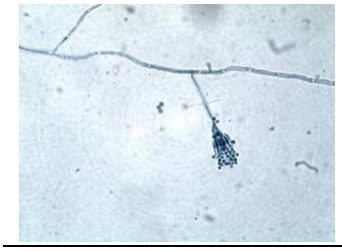	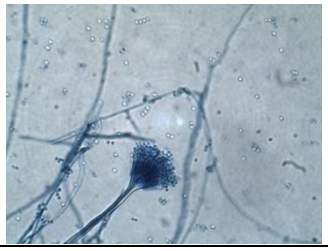	

2.2 Image Processing

The pre-processing stage is important in modifying the raw image to be use in the next stage [14]. It is a simple process of modifying the pixel brightness of an image. In this case, the raw RGB image of fungi undergoes a grayscale transformation. The process is done to eliminate the hue and saturation values of the original RGB image. The image is transformed to ease the image enhancement processes in the next step. Plus, the grayscale image which is represented in the form of unsigned 8-bit integers (uint8) is then converted into a double precision form which rescales the output from integer data types from [0,255] to the range (0,1). The conversion is done as to ease the calculation of the standard deviation, σ (contrast) and mean, μ (brightness) of the image in the proposed technique of adaptive gamma correction and fuzzy logic. The process implemented in this study is summarized as in Figure 2.

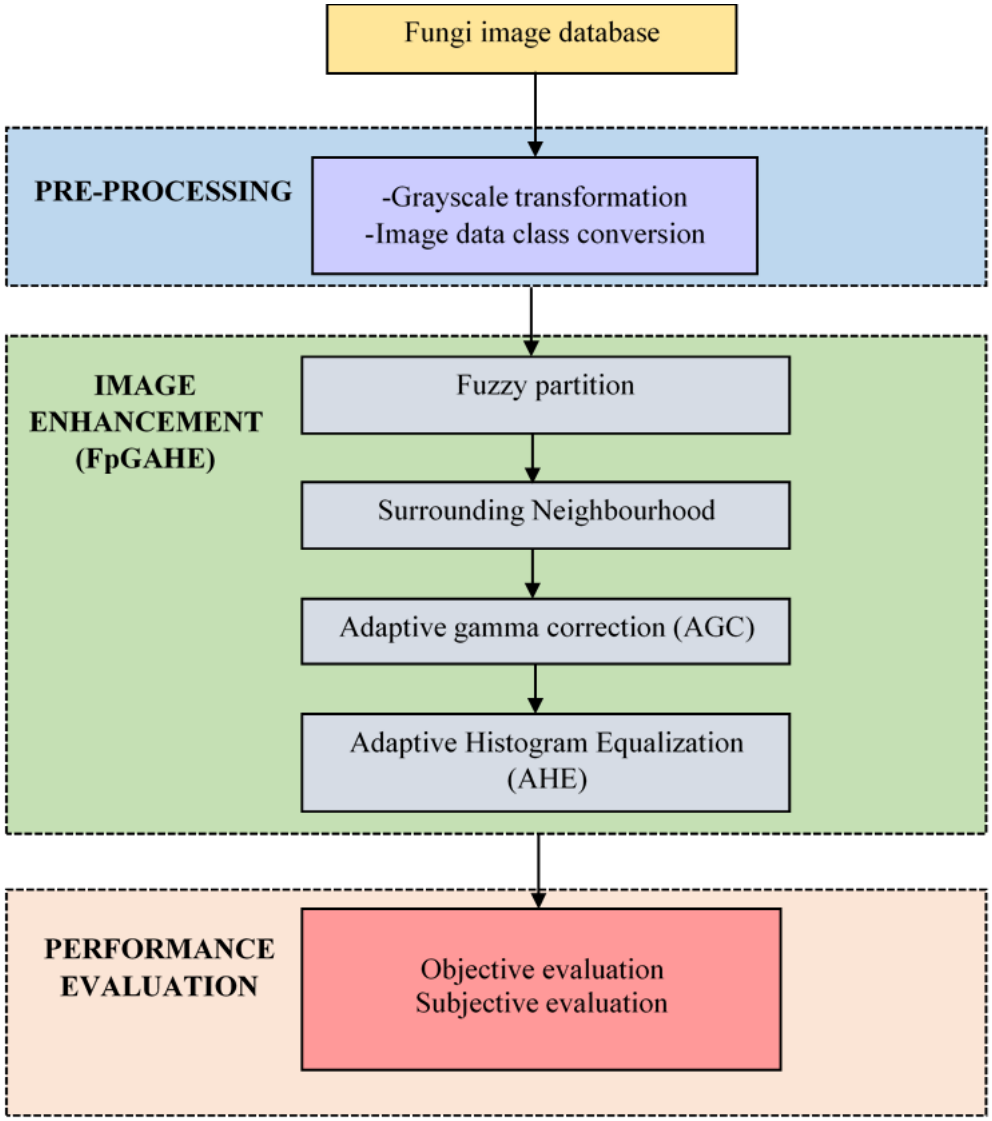

Fig. 2. The implementation steps in microscopic image processing

2.2.1 Adaptive histogram equalization

The goal of this enhancement is to enhance the structure of fungi while keeping a minimal exposure of the surrounding noise [15,16]. The comparison can be seen as shown in Figure 3. It is found that the technique of adaptive histogram equalization produces the most satisfactory result among the other two. This technique enhances the structure of fungi while keeping a low exposure of noise in the image. The technique of HE causes the fungi to lose its structure as the image becomes too dark. For CLAHE, although the structure of fungi is enhanced, the surrounding noise is also enhanced which can cause some difficulties in image segmentation later.

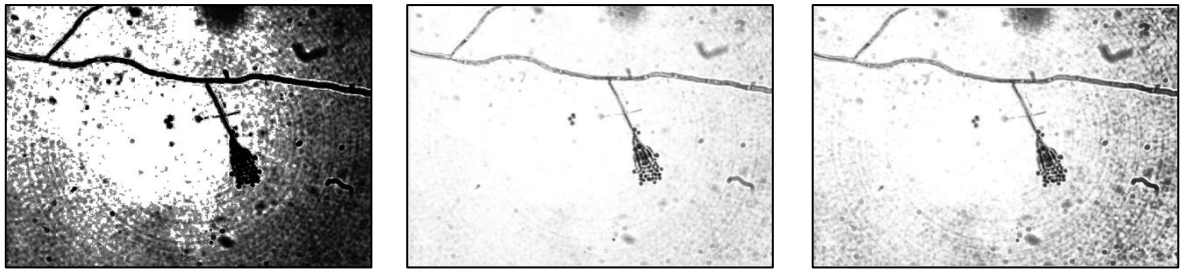

(a) (b) (c)

Fig. 3. Comparison of different method on microscopic image of fungi (a) HE (b) AHE (c) CLAHE

2.2.2 Adaptive gamma correction

Although the image has been enhanced, a satisfactory result is not yet achieved. As can be seen in Figure 3, the structure of fungi needs to be further enhanced to see its structure more clearly. Due to this, the technique of adaptive gamma correction (AGC) is applied [17,18]. AGC is derived from the original technique of gamma correction which aims to increase the contrast of an image without degrading its quality. In the original technique of AGC, both low contrast and high contrast images are considered [19]. However, in this study, only the technique for low contrast images is used. This is to match the characteristic of the microscopic image which are low in contrast.

The technique works by classifying the image into the characteristic of bright and dark image using the mean intensity (μ) of pixel values in the image. The bright image has a mean intensity value of $\mu > 0.5$ while the dark image has a value of $\mu < 0.5$. AGC is applied on the images by using a transformation function with a specific value of gamma. The value of gamma (γ) is obtained based on power-law transformation curve [20].

To determine the best gamma value for both the bright and dark images, different values are tested on various type of fungi image. The values are also tested on images ranging from different level of brightness. The value of gamma is then selected based on the value that produces the best result. In this study, for bright image the value of gamma used is $\gamma = 2.3$ while for dark image, $\gamma = 1.3$. Both values are obtained after trying out numerous values. A different function and gamma value are applied based on the class of image. This means that for bright image, the characteristic that follows is the mean intensity must be $\mu > 0.5$. Thus, the gamma value used is 2.3. The transformation function used for this image is as follows;

$$I_{out} = I_{in}^{\gamma} \tag{1}$$

where I_{out} is the output image intensity, I_{in} is the input image intensity, γ is gamma value. The result of the transformation is shown as in Figure 4(b). Figure 4(c) shows the combination of AHE technique together with adaptive gamma correction (AGC) transformation.

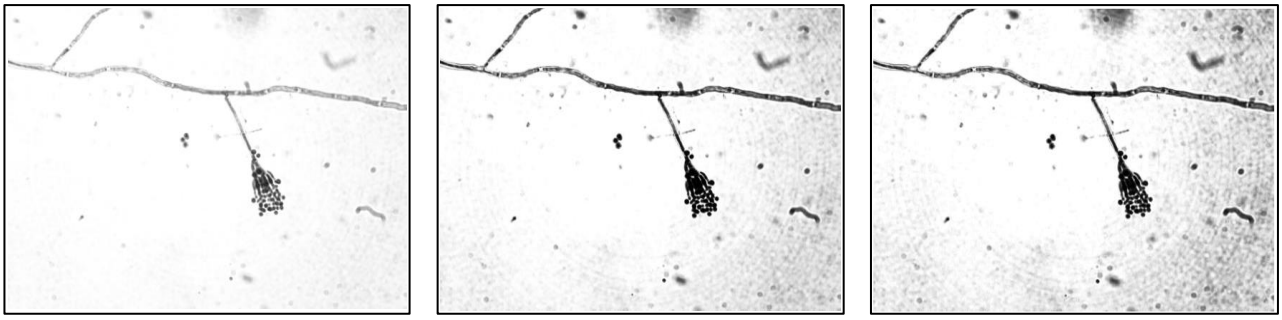

(a) (b) (c)

Fig. 4. Bright fungi image (a) Original grayscale (b) AGC transformation (c) Combination of AHE and AGC transformation

For dark image the characteristic is that the mean intensity is μ < 0.5. Thus, the gamma value that is applied in the transformation function is 1.3. The transformation function used for dark image is as follows;

$$I_{out} = \frac{I_{in}^{\gamma}}{I_{in}^{\gamma}+(1-I_{in}^{\gamma})\times\mu^{\gamma}} \quad (2)$$

where μ is the mean intensity of the image. The result of the transformation for dark image is as shown in Figure 5.

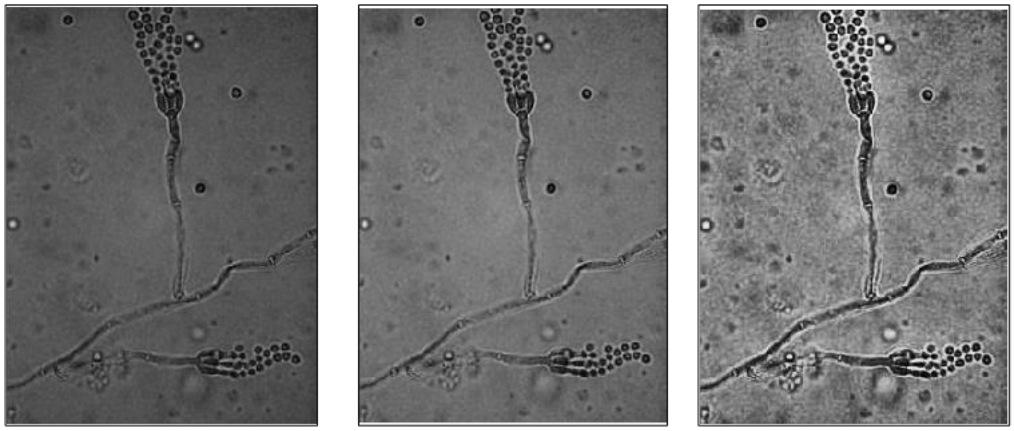

(a) (b) (c)

Fig. 5. Dark fungi image (a) Original grayscale (b) AGC transformation (c) Combination of AHE and AGC transformation

However, since the contrast of the fungi image database might vary, a high contrast image is also taken into consideration. Thus, fuzzy logic is implemented together with the AGC technique to also consider the contrast together with the brightness of an image.

2.2.3 Fuzzy-partition gamma adaptive histogram equalization (stage 1: fuzzy partition)

In creating a fuzzy partition, the type of membership function needs to be determined. In this case, the proposed method implements the membership function curve of triangular curve as it is easier to partition a fuzzy region using a triangular curve as it has a clear peak point. Plus, the accurate value of each point in a triangular curve is easier to calculate.

Subsequently, the process of partitioning is done by separating the triangular membership functions into several fuzzy regions. In order to carry out the process of partitioning, the input variables i.e., brightness and contrast are considered [21]. The first variable which is brightness, μ, is divided into sets of very dark, dark, medium, bright and very bright ranging over the value of 0 to 1. The brightness of an image differs depending on the value of mean which is signified as follows;

$$\mu = \frac{1}{N}\sum_{i,j} I_{(i,j)} \tag{3}$$

where *N* is the total number of pixel and $I_{(i,j)}$ is the pixel gray level value at position *(i,j)*.

Meanwhile, the second variable which is contrast, σ is also divided into sets of very low, low, medium, high and very high ranging over the value of 0 to 0.5. The value of σ can be obtained as follows;

$$\sigma = x_{max} - x_{min} \tag{4}$$

In order to interpret the fuzzy set rules, the Mamdani model was utilized. Seven different rules were applied to characterize the fuzzy rules as shown in Table 2.

Table 2
If- then rules

	Inputs		**Output**
Rules	*A* (Brightness)	*B* (Contrast)	*C* (Intensity)
Rule 1	Low	Low	Bright
Rule 2	Low	High	Dark
Rule 3	Moderate	Moderate	Moderate
Rule 4	Moderate	Low	Bright
Rule 5	Moderate	High	Dark
Rule 6	High	High	Dark
Rule 7	High	Low	Bright

Let Q = {A_1,A_2,….,A_n} a family of fuzzy sets on a universe of the discourse Z. Y is a fuzzy partition of Z if;

$$\forall A_i \in Q \exists x \in Z : A_i(x) \neq 0 \tag{5}$$

$$\sum_{i=1}^{n} A_i(x) = 1 \forall x \in Z \tag{6}$$

The fuzzy partition Q is composed of five fuzzy sets Q = {A_1,A_2,….,A_5} which are labelled based on the sets of input variables. It is defined by triangular fuzzy sets whose membership function is denoted as follows;

$$A_i(x) = \begin{cases} 0, & x < x_{i-1} \\ \frac{x - x_{i-1}}{h}, & x_{i-1} \leq x \leq x_i \\ \frac{x_{i+1} - x}{h}, & x_i \leq x \leq x_{i+1} \\ 0, & x > x_{i+1} \end{cases} \quad (7)$$

where $x_0 = x_{min}$, $x_i = x_{i-1} + h$ and $h = (x_{max} - x_{min}) / (n\text{-}1)$.

After determining both the variables and number of sets, the process of partitioning can be done. The first variable which is brightness is divided into sets of very dark, dark, medium, bright and very bright ranging over the value of zero to one. Next, the second variable which is contrast is also divided into sets of very low, low, medium, high and very high ranging over the value of zero to 0.5. The regions of the sets are then developed by dividing the membership function based on the meeting point between one peak of the triangular curve to another. However, the value of each triangular peak must be determined initially to determine the value of the regions. The value of each peak was obtained as follow;

$$p = \frac{x}{N} \quad (8)$$

where p is the peak value, x is highest value of brightness or contrast, and N is the number of peaks. Then, the value of the meeting point between the peaks were calculated as follows;

$$m_p = \left(\frac{p_2 - p_1}{2}\right) + p_1 \quad (9)$$

where m_p is the value of the meeting point between two peaks, p_1 is the first peak value and p_2 is the second peak value.

The range of each region is also based on the value of each meeting point between the peaks as shown in Figure 6.

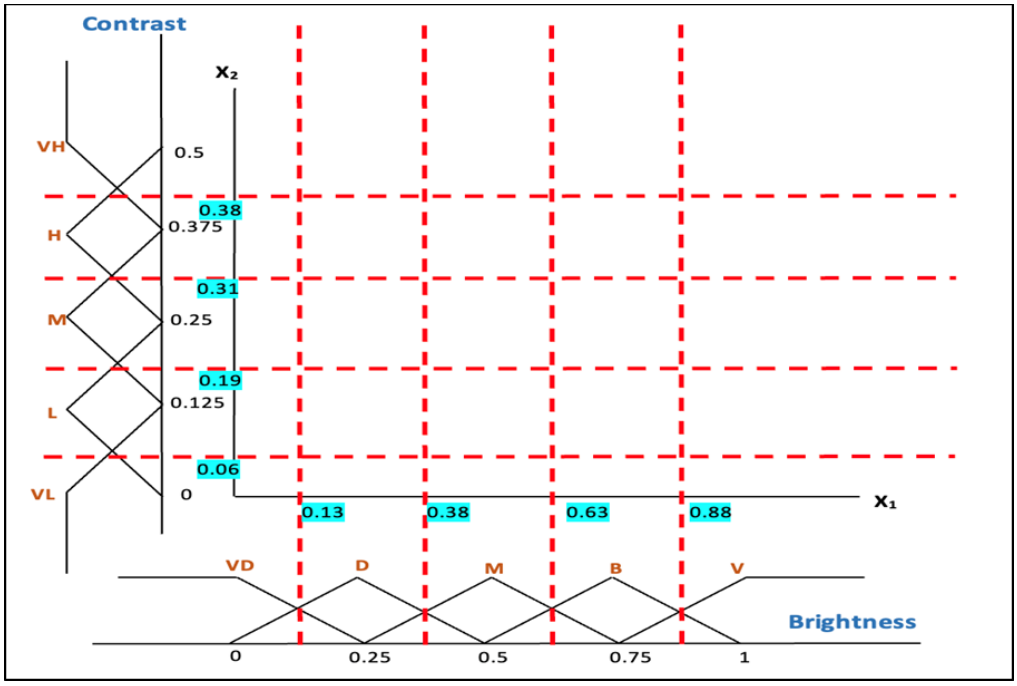

Fig. 6. Membership function partitioning

A total of 25 sets are obtained through the process of partition as tabulated in Table 3. These sets will be observed later to see which region contains the most amount of data.

Table 3
Sets of Fuzzy Partition

Set	Brightness	Contrast
Set 1	0.00 – 0.13	0.00 – 0.06
Set 2	0.13 – 0.38	0.00 – 0.06
Set 3	0.38 – 0.63	0.00 – 0.06
Set 4	0.63 – 0.88	0.00 – 0.06
Set 5	0.88 – 1.00	0.00 – 0.06
Set 6	0.00 – 0.13	0.06 – 0.19
Set 7	0.13 – 0.38	0.06 – 0.19
Set 8	0.38 – 0.63	0.06 – 0.19
Set 9	0.63 – 0.88	0.06 – 0.19
Set 10	0.88 – 1.00	0.06 – 0.19
Set 11	0.00 – 0.13	0.19 – 0.31
Set 12	0.13 – 0.38	0.19 – 0.31
Set 13	0.38 – 0.63	0.19 – 0.31
Set 14	0.63 – 0.88	0.19 – 0.31
Set 15	0.88 – 1.00	0.19 – 0.31
Set 16	0.00 – 0.13	0.31 – 0.38
Set 17	0.13 – 0.38	0.31 – 0.38
Set 18	0.38 – 0.63	0.31 – 0.38
Set 19	0.63 – 0.88	0.31 – 0.38
Set 20	0.88 – 1.00	0.31 – 0.38
Set 21	0.00 – 0.13	0.38 – 0.50
Set 22	0.13 – 0.38	0.38 – 0.50
Set 23	0.38 – 0.63	0.38 – 0.50
Set 24	0.63 – 0.88	0.38 – 0.50
Set 25	0.88 – 1.00	0.38 – 0.50

By employing the rule of extraction in Table 3, an example distributed values of input variables for single image of *Penicillium sp.* is presented in Figure 7. From 25 regions, from the observation of the data distribution over the 25 fuzzy regions, only 4 regions are occupied with data. By observing Figure 7, it is perceived that the region of brightness between 0.63 and 0.88 and contrast from 0.06 to 0.19 dominates with a total number of 88 data.

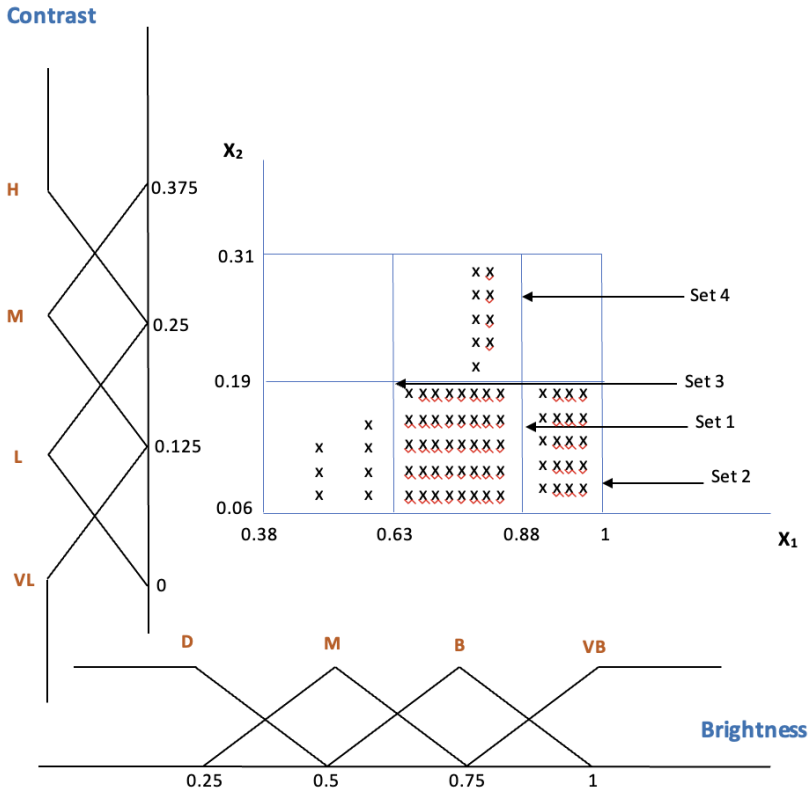

Fig. 7. Example of distribution of image data for single image of *Penicillium sp.*

This set is then labelled as Set 1. Subsequently, each occupied region is labelled as Set 2, Set 3 and Set 4. The sets along with the range of brightness and contrast and the number of data are specified as in Table 4.

Table 4
Fuzzy Partition for Selected Set

Set	Brightness	Contrast	No. of data
Set 1	0.63 – 0.88	0.06 – 0.19	88
Set 2	0.88 – 1.00	0.06 – 0.19	35
Set 3	0.38 – 0.63	0.06 – 0.19	7
Set 4	0.63 – 0.88	0.19 – 0.31	9

2.2.4 Fuzzy-partition gamma adaptive histogram equalization (stage 2: surrounding neighbourhood)

In real application, the distributed of crisps values data are not homogenous or from the same class and this may cause a significant deterioration in image enhancement. To solve the distribution of the data in each set, a SN is introduced to utilize the distances and distributions of the data before defuzzification process [23]. Here, a centroid point is investigated to reduce the bias information in distributed data.

To obtain the value of the centroids, the query point must be determined first. By using the data available in each set of partition, the value of the query point, v, is determined. The query point plays an important role in determining the values of nearest centroid surrounding neighbours that will be used later in obtaining the value of gamma. For each four different set of partition, the value of the

query point will be different. Thus, the value of the query point is obtained by computing the mean of the data in each partition and is interpreted as;

$$v = \frac{\sum b}{N} \tag{10}$$

where *v* is the query point, *b* is the values of data sample and *N* is the amount of data in a partition.

Subsequently, the distance between the query point and the data sample is calculated. It is defined as;

$$d = \|v - b\| \tag{11}$$

where *d* is the distance between the query point and the data sample, *b* is the data sample and *v* are the query point.

The first centroid surrounding neighbour is obtained by determining the data sample that is located the closest to the query point by using Eq. (11). The first nearest centroid neighbour is then labelled as x_1. Next, the following nearest centroid surrounding neighbours is determined by calculating the centroid of the remaining data samples. The previous data sample that has been chosen as the first nearest centroid surrounding neighbour is omitted from this process. Thus, the centroid of a set of data samples,x_{rj}^{c}, can be obtained by using the equation below;

$$b_r^c = \frac{(\sum_{r=1}^{r-1} x_r) + b}{r} \tag{12}$$

The nearest centroid surrounding neighbour is obtained by calculating the shortest distance between the centroid of a set of data samples and the query point which is denoted as follows;

$$x_r = min\|(v - b_r^c)\| \tag{13}$$

The value of the second centroid of a set of data samples is obtained by using Eq. (14) when applying Eq. (12) with the value of *r*=2.

$$b_2^c = \frac{x_1 + b}{2} \tag{14}$$

Therefore, the second centroid surrounding neighbour can be denoted as;

$$x_2 = \min\|v - b_2^c\| \tag{15}$$

Subsequently, for the value of the third centroid, the procedure is reiterated by obtaining the centroid between the data samples and the previous nearest centroid neighbours. A new equation derived from Eq. (10) is formed. Thus, Eq. (16) is obtained as follows;

$$b_3^c = \frac{x_1 + x_2 + b}{3} \tag{16}$$

Based on Eq. (7), the equation for the third centroid surrounding neighbour is determined as follows;

$$x_3 = \min\|(v - b_3^c)\| \quad (17)$$

The process of centroid SN is concluded when three values of the centroid surrounding neighbour is obtained. This is because the three values are adequate to be used in the next step.

3. Results

In this paper the performance evaluation is presented into subjective and objective evaluations. Subjective evaluation is visually observed by human while objective evaluation used an algorithm to measure the image quality. The experiments have been executed in Matlab R2017a by using a computer with the specifications of Intel Core i7, 1.80 GHz CPU, 8G RAM and the Windows 10 operating system. The experiments were run in two types of databases i.e., clean image and corrupted image with salt and pepper noise and Gaussian noise as in Table 5.

Table 5
Example of Clean and Corrupted FpGAHE Enhanced Image

Clean condition	**Salt and pepper noise**	**Gaussian noise**
Penicillium		
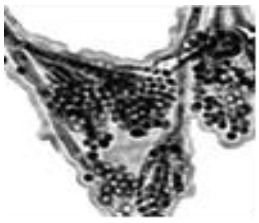		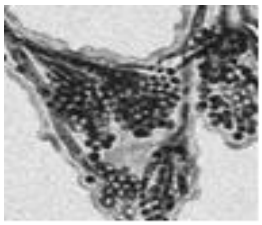
A. terreus		
	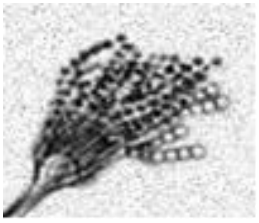	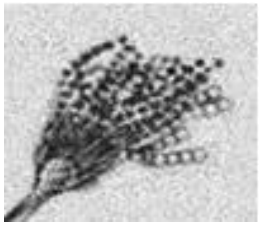
A. fumigatus		
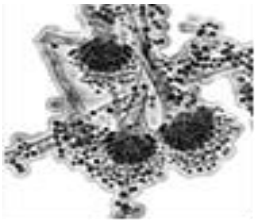	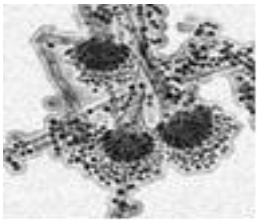	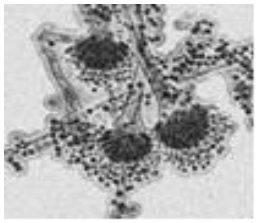

3.1 Performance Evaluation Based on Subjective Evaluation

The subjective evaluation is evaluated based on the observation of enhanced image in term of textures, shapes and colours. The proposed technique of FpGAHE was compared with five other existing image enhancement techniques i.e., HE, AHE, CLAHE, gamma correction (GC) and AGC. As can be seen in Table 6, the experimental results demonstrate from the existing image enhancement techniques, AHE exhibited the best result. However, the textures of the *A. terreus* were not clear and

the background of image was not uniform. Meanwhile, the HE and AGC was not well practicable and the results were still undesirable where many false textures were generated. From the result, the technique of CLAHE showed the least desirable result for the species of *Penicillium* as the background noise is still present causing the structure to be unclear. Subsequently, the technique of GC produced output images that is quite low in contrast which causes some features of fungi to be indistinct or disappear as seen on *A. terreus*. In comparison with the existing techniques, the results by FpGAHE exhibits visually better quality. In addition, the enhanced image by the FpGAHE was more convincing where that the vein and features of fungi was presented clearly.

Table 6
Performance of Subjective Evaluations (Clean Condition)

FpGAHE	HE	AHE	CLAHE	GC	AGC
Penicillium					
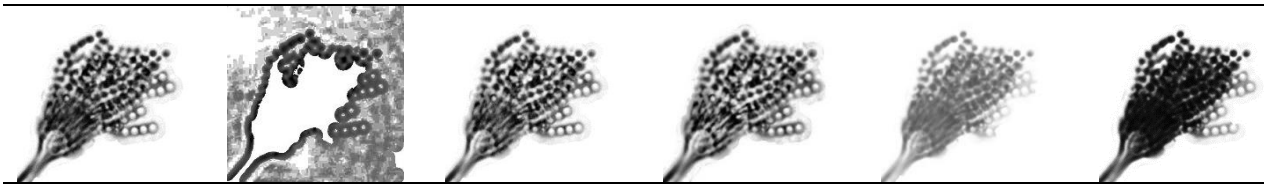					
A. terreus					
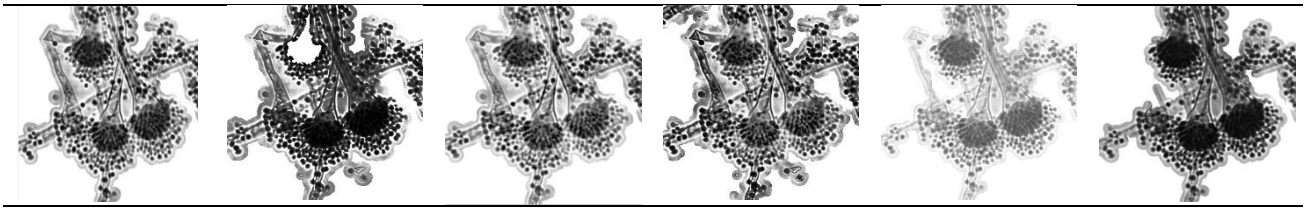					
A. fumigatus					

Table 7 and 8 showed the enhanced image when it was corrupted with salt and pepper noise and Gaussian noise respectively. By using the HE and AGC, the image is not correctly enhanced and segmented. In fact, the texture cannot be detected at all when the image affected severely by the noise. This discourages the use of AGC to produce desirable images output. On the other hand, it was observed that the techniques of AHE and CLAHE presented better performance than HE and AGC. However, for some of the species such as *A. fumigatus*, the structure was slightly blur and the texture was barely unseen when the image was corrupted.

Table 7
Performance of Subjective Evaluations (Salt and Pepper Noise)

FpGAHE	HE	AHE	CLAHE	GC	AGC
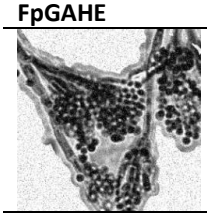	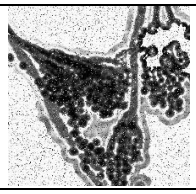		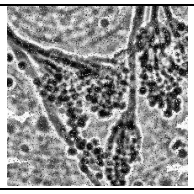	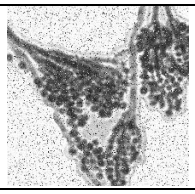	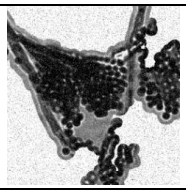
Penicillium					
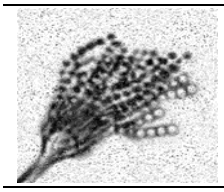	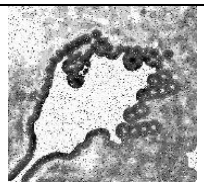	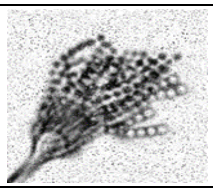	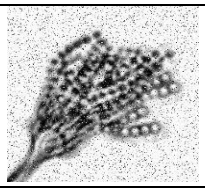	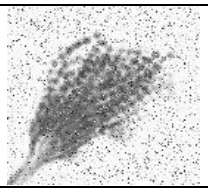	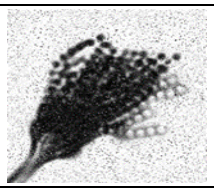
A. terreus					
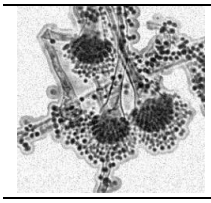	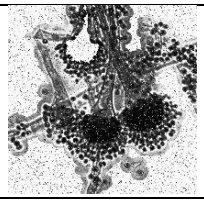	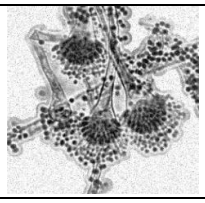	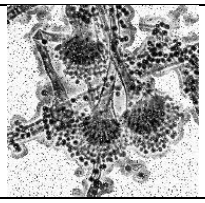	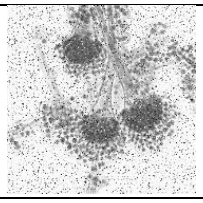	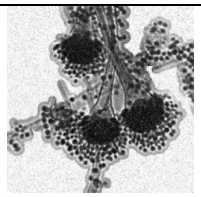
A. fumigatus					

For the technique of GC, it is deduced that this technique produced the most unsatisfactory result. It is observed that the structure of fungi became unclear and indistinct for both corrupted noise condition of salt and pepper and Gaussian noise. Meanwhile, the proposed technique of FpGAHE can deal with spatially varying blur and eliminate noise effect. However, the image for *Penicillium* was not clear.

Table 8
Performance of Subjective Evaluations (Gaussian Noise)

FpGAHE	HE	AHE	CLAHE	GC	AGC
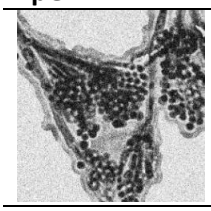			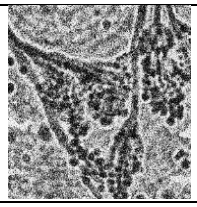	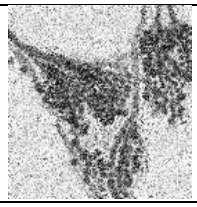	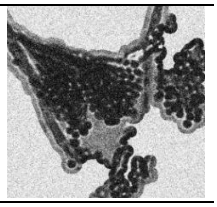
Penicillium					
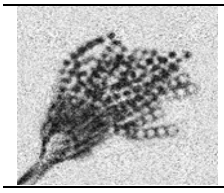	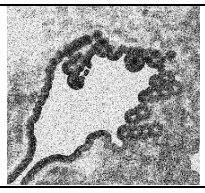	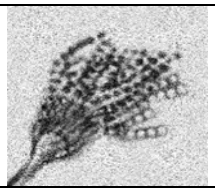	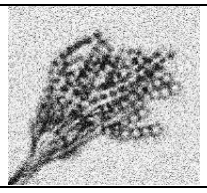	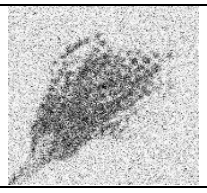	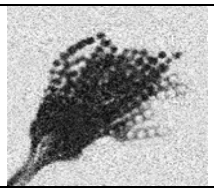
A. terreus					
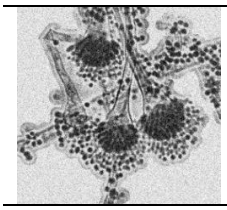	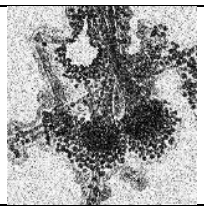	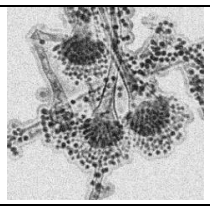	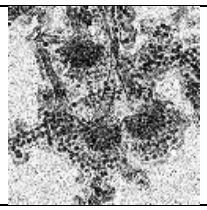	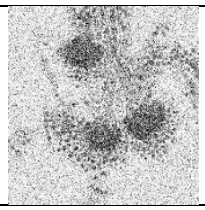	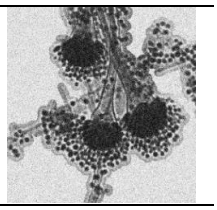
A. fumigatus					

3.2 Performance Evaluation Based on Objective Evaluation

The performance evaluation is divided into two i.e., image processing and image classification. In image processing, four image quality assessment (IQA) methods namely peak signal to noise ratio (PSNR), mean square error (MSE), structured similarity indexing method (SSIM) and feature similarity indexing method (FSIM) were used for the objective evaluation. In order to determine the effectiveness of the proposed technique, the evaluations of FpGAHE were compared with other image enhancement techniques i.e., HE, AHE, CLAHE, GC and AGC.

In image classification, five nearest neighbour classifiers which are k Nearest Neighbour (kNN), k Nearest Centroid Neighbourhood (kNCN), Fuzzy k Nearest Neighbour (FkNN), Fuzzy-Based k Nearest Centroid Neighbour (FkNCN) and Improved Fuzzy-Based k Nearest Centroid Neighbour (IFkNCN) are employed [11]. Here, the portion of training and testing number has been divided into 70% and 30%, respectively. The empirical comparisons in term of the classification accuracy (CA) rate are considered.

3.2.1 Performance evaluation based on image processing

The summary of the results for clean and noise corrupted images based on IQA method is provided in Table 9, 10 and 11 respectively. The yellow, grey, green, and blue rectangle filled indicate the best performance in each species for PSNR, MSE, SSIM and FSIM respectively. Based on the tables, there are some interesting points that are observed and obtained. Firstly, the performance of the IQA methods in clean condition exhibit the best results compared to noise corrupted environment. Next, from Table 9, 10 and 11, it is observed that the proposed technique of FpGAHE exhibited better results in comparison with the other five existing techniques. However, the technique of AHE presented the best result for *Penicillium* for the SSIM evaluation in clean condition.

Table 9
Performance of Clean Image Based on Image Processing

IQA	Fungi	HE	AHE	CLAHE	GC	AGC	FpGAHE
PSNR	*Penicillium*	29.037	29.815	28.920	29.649	29.763	29.862
	A. terreus	26.742	33.682	31.195	34.817	34.899	37.018
	A. fumigatus	26.333	27.444	27.265	26.775	27.434	27.556
MSE	*Penicillium*	81.814	68.484	84.043	71.981	69.290	67.730
	A. terreus	150.46	49.278	49.768	41.173	39.359	24.570
	A. fumigatus	152.46	126.64	123.03	137.73	126.29	124.67
SSIM	*Penicillium*	0.8595	0.9199	0.8367	0.8665	0.8690	0.8948
	A. terreus	0.3934	0.5404	0.5453	0.5477	0.5652	0.6146
	A. fumigatus	0.8347	0.8876	0.8632	0.8516	0.8796	0.8894
FSIM	*Penicillium*	0.9061	0.9313	0.8839	0.9115	0.9206	0.9328
	A. terreus	0.6636	0.8063	0.7607	0.8050	0.8133	0.8544
	A. fumigatus	0.8962	0.9452	0.9323	0.9219	0.9375	0.9458

Subsequently, it is seen in Table 10 and 11 that AHE outperformed in salt and pepper and Gaussian noise in PSNR and MSE for the species of *A. fumigatus* and *A. terreus* respectively. However, the result obtained shows that AHE was a bit superior compared to FpGAHE with a difference of less than 0.1 and 10 for both PSNR and MSE. Lastly, the proposed technique of FpGAHE exhibited better results than the other image enhancement techniques for both clean condition and noise corrupted condition. The results also show that HE and CLAHE performs the worst for the species of *A. terreus*

and *Penicillium* respectively by obtaining the lowest result in both of the clean and noise corrupted conditions.

Table 10
Performance of Salt and Pepper Noise Corrupted, Image Based on Image Processing

IQA	Fungi	HE	AHE	CLAHE	GC	AGC	FpGAHE
PSNR	*Penicillium*	27.896	28.608	27.824	28.475	28.598	28.878
	A. terreus	25.569	28.962	28.811	28.755	28.896	29.107
	A. fumigatus	27.240	27.622	27.474	27.093	27.590	27.553
MSE	*Penicillium*	106.39	90.318	108.16	93.393	90.527	84.884
	A. terreus	181.78	86.185	86.171	87.293	88.068	82.894
	A. fumigatus	123.74	115.37	117.25	127.98	116.29	117.07
SSIM	*Penicillium*	0.0446	0.0575	0.0427	0.0458	0.0480	0.0586
	A. terreus	0.0370	0.0598	0.0502	0.0503	0.0506	0.0632
	A. fumigatus	0.1629	0.1888	0.1638	0.1578	0.1671	0.1898
FSIM	*Penicillium*	0.6529	0.7088	0.6392	0.6498	0.6561	0.7250
	A. terreus	0.6584	0.7451	0.7033	0.7022	0.7062	0.7600
	A. fumigatus	0.7646	0.7887	0.7707	0.7530	0.7746	0.7948

For the technique of GC, this technique underperforms for the species of *A. fumigatus* in both of the noise corrupted conditions. In a nutshell, the FpGAHE technique provides a good alternative to image enhancement over the existing techniques as it gives the lowest value of MSE and the highest value of PSNR, SSIM and FSIM.

Table 11
Performance of Gaussian Noise Corrupted, Image Based on Image Processing

IQA	Fungi	HE	AHE	CLAHE	GC	AGC	FpGAHE
PSNR	*Penicillium*	27.851	27.944	27.794	27.888	27.922	28.045
	A. terreus	25.982	27.776	27.539	27.485	27.577	27.661
	A. fumigatus	27.390	27.493	27.417	27.266	27.492	27.566
MSE	*Penicillium*	107.49	105.22	108.92	106.57	105.70	102.81
	A. terreus	165.30	109.57	115.77	116.93	114.99	112.61
	A. fumigatus	119.52	117.33	118.87	122.99	117.55	115.42
SSIM	*Penicillium*	0.0383	0.0425	0.0374	0.0391	0.0407	0.0426
	A. terreus	0.0209	0.0304	0.0265	0.0250	0.0274	0.0305
	A. fumigatus	0.1310	0.1432	0.1326	0.1213	0.1377	0.1470
FSIM	*Penicillium*	0.6681	0.7160	0.6599	0.6705	0.6717	0.7273
	A. terreus	0.6975	0.7519	0.7379	0.7251	0.7417	0.7611
	A. fumigatus	0.7641	0.7846	0.7677	0.7459	0.7737	0.7899

3.2.2 Performance evaluation based on image classification

The empirical comparisons based on image classification is presented in Table 12, 13 and 14. The yellow rectangle filled indicate the highest CA for clean condition, salt and pepper and Gaussian noises, respectively. It is observed that IFkNCN consistently outperformed the kNN, kNCN and FkNN and FkNCN in different noises condition. However, at clean condition, FkNCN were seen comparable and a little bit superior to the IFkNCN with a difference of less than 0.5%. Nevertheless, as the images are corrupted in different noises, the IFkNCN performed significantly the best. In term of image processing technique, the results show that the HE exhibited the lowest CA when the image is in clean condition and corrupted with salt and pepper noise and tested with kNN. However, for the

Gaussian noise corrupted condition, GC exhibited the lowest CA when tested with kNN, kNCN, FkNN, FkNCN and IFkNCN. Next, it was found for HE, AHE, CLAHE, GC, AGC and FpGAHE, the results are outperformed when the features were tested using IFkNCN. It is also noticeable that the proposed technique of FpGAHE performed better than the existing image enhancement techniques under all classifiers. Lastly, the results show the CA for FpGAHE outperformed for both clean and corrupted images.

Table 12
Performance of Clean Image Based on Image Classification

	HE	AHE	CLAHE	GC	AGC	FpGAHE
kNN	85.27	91.42	87.05	88.48	91.47	93.45
kNCN	86.01	93.68	87.46	88.69	92.58	95.22
FkNN	86.39	94.02	88.13	89.03	92.36	94.09
FkNCN	86.95	94.68	88.43	89.38	94.42	95.93
IFkNCN	87.34	94.38	88.78	90.04	94.72	95.58

Table 13
Performance of Salt and Pepper Noise Corrupted Image, Based on Image Classification

	HE	AHE	CLAHE	GC	AGC	FpGAHE
kNN	75.91	89.97	77.00	76.32	88.21	92.12
kNCN	76.01	90.35	77.13	76.54	89.73	91.83
FkNN	76.07	91.38	77.21	76.60	89.75	92.12
FkNCN	76.34	91.94	77.40	76.86	91.09	92.57
IFkNCN	76.46	91.74	77.76	76.98	91.47	92.59

Table 14
Performance of Gaussian Noise Corrupted Image, Based on Image Classification

	HE	AHE	CLAHE	GC	AGC	FpGAHE
kNN	74.47	88.16	75.22	73.06	89.52	90.52
kNCN	74.98	90.51	75.40	74.12	87.97	91.57
FkNN	75.00	89.97	75.60	74.49	88.42	90.12
FkNCN	75.12	91.71	75.92	74.76	90.12	93.64
IFkNCN	75.36	92.43	75.78	74.90	90.64	93.95

4. Conclusions

The nature of a microscopic image of fungi is usually low in contrast. Hence, it is important to find an image enhancement technique that can increase and alter the contrast of a fungi image without degrading its quality. This paper presents a new approach, fuzzy-partition gamma adaptive histogram equalization (FpGAHE) instils the method of fuzzy partition by combining it with the existing image enhancement technique of adaptive histogram equalization (AHE) and adaptive gamma correction (AGC). The proposed image enhancement technique was tested on two different species of fungi, *Penicillium* and *Aspergillus*. The result obtained suggest that FpGAHE has a better performance in terms of both subjective and objective evaluation. Subsequently, *A. terreus* outperforms in most of the experiments.

Acknowledgement
The authors would like to thank the Faculty of Electrical Engineering & Technology, Universiti Malaysia Perlis for providing the facilities and financial support under FKTE Research Activities Fund.

References

[1] Dufresne, Simon Frédéric, Kieren A. Marr, and Shmuel Shoham. "Diagnosis of systemic fungal diseases." *Principles and practice of transplant infectious diseases* (2019): 819-840. https://doi.org/10.1007/978-1-4939-9034-4_48

[2] Diba, K., P. Kordbacheh, S. H. Mirhendi, S. Rezaie, and M. Mahmoudi. "Identification of Aspergillus species using morphological characteristics." *Pakistan journal of medical sciences* 23, no. 6 (2007): 867.

[3] Larone, Davise H. "Medically important fungi." *Revista do Instituto de Medicina Tropical de São Paulo* 36 (1994): 432-432. https://doi.org/10.1590/S0036-46651994000500016

[4] Sugui, Janyce A., Kyung J. Kwon-Chung, Praveen R. Juvvadi, Jean-Paul Latgé, and William J. Steinbach. "Aspergillus fumigatus and related species." *Cold Spring Harbor perspectives in medicine* 5, no. 2 (2015). https://doi.org/10.1101/cshperspect.a019786

[5] Agarwal, Ritesh, and Dheeraj Gupta. "Severe asthma and fungi: current evidence." *Medical mycology* 49, no. Supplement_1 (2011): S150-S157. https://doi.org/10.3109/13693786.2010.504752

[6] Ehgartner, Daniela, Christoph Herwig, and Jens Fricke. "Morphological analysis of the filamentous fungus Penicillium chrysogenum using flow cytometry—the fast alternative to microscopic image analysis." *Applied Microbiology and Biotechnology* 101 (2017): 7675-7688. https://doi.org/10.1007/s00253-017-8475-2

[7] Zabani, Farah Nabilah, Haryati Jaafar, Nur Rodiatul Raudah Mohamed Radzuan, and Aimi Salihah Abdul Nasir. "Preliminary Studies for Detection of Penicillium Species Using Adaptive Histogram Equalization Technique." In *2019 IEEE 9th International Conference on System Engineering and Technology (ICSET)*, pp. 236-240. IEEE, 2019. https://doi.org/10.1109/ICSEngT.2019.8906499

[8] Mustafa, Wan Azani, Haniza Yazid, and Mastura Jaafar. "A systematic review: Contrast enhancement based on spatial and frequency domain." *Journal of Advanced Research in Applied Mechanics* 28, no. 1 (2016): 1-8.

[9] Acharya, Upendra Kumar, and Sandeep Kumar. "Genetic algorithm based adaptive histogram equalization (GAAHE) technique for medical image enhancement." *Optik* 230 (2021): 166273. https://doi.org/10.1016/j.ijleo.2021.166273

[10] Magudeeswaran, V., and J. Fenshia Singh. "Contrast limited fuzzy adaptive histogram equalization for enhancement of brain images." *International Journal of Imaging Systems and Technology* 27, no. 1 (2017): 98-103. https://doi.org/10.1002/ima.22214

[11] Wong, Ooi Qun, and Parvathy Rajendran. "Image segmentation using modified region-based active contour model." *J. Eng. Appl. Sci* 14 (2019): 5710-5718. https://doi.org/10.36478/jeasci.2019.5710.5718

[12] Dhanachandra, Nameirakpam, and Yambem Jina Chanu. "An image segmentation approach based on fuzzy c-means and dynamic particle swarm optimization algorithm." *Multimedia tools and applications* 79, no. 25-26 (2020): 18839-18858. https://doi.org/10.1007/s11042-020-08699-8

[13] Versaci, Mario, and Francesco Carlo Morabito. "Image edge detection: A new approach based on fuzzy entropy and fuzzy divergence." *International Journal of Fuzzy Systems* 23, no. 4 (2021): 918-936. https://doi.org/10.1007/s40815-020-01030-5

[14] Abdulah, Cik Siti Khadijah, Mohamad Nur Khairul Hafizi Rohani, Baharuddin Ismail, Mohd Annuar Mohd Isa, Afifah Shuhada Rosmi, Wan Azani Wan Mustafa, Ahmad Zaidi Abdullah, Wan Nor Munirah Ariffin, and Mohamad Kamarol Mohd Jamil. "Review Study of Image De-Noising on Digital Image Processing and Applications." *Journal of Advanced Research in Applied Sciences and Engineering Technology* 30, no. 1 (2023): 331-343. https://doi.org/10.37934/araset.30.1.331343

[15] Jebadass, J. Reegan, and P. Balasubramaniam. "Low contrast enhancement technique for color images using interval-valued intuitionistic fuzzy sets with contrast limited adaptive histogram equalization." *Soft Computing* 26, no. 10 (2022): 4949-4960. https://doi.org/10.1007/s00500-021-06539-x

[16] Jebadass, J. Reegan, and P. Balasubramaniam. "Low light enhancement algorithm for color images using intuitionistic fuzzy sets with histogram equalization." *Multimedia Tools and Applications* 81, no. 6 (2022): 8093-8106. https://doi.org/10.1007/s11042-022-12087-9

[17] Swarup, Jyoti, and Indu Sreedevi. "DWT based historical image enhancement technique using adaptive gamma correction." *Journal of Algebraic Statistics* 13, no. 1 (2022): 654-664.

[18] Qi, Min, Shanshan Cui, Xin Chang, Yuelei Xu, Hongying Meng, Yi Wang, and Ting Yin. "Multi-region nonuniform brightness correction algorithm based on L-channel gamma transform." *Security and Communication Networks* 2022 (2022). https://doi.org/10.1155/2022/2675950

[19] Rahman, Shanto, Md Mostafijur Rahman, Mohammad Abdullah-Al-Wadud, Golam Dastegir Al-Quaderi, and Mohammad Shoyaib. "An adaptive gamma correction for image enhancement." *EURASIP Journal on Image and Video Processing* 2016, no. 1 (2016): 1-13. https://doi.org/10.1186/s13640-016-0138-1

[20] Qian, Shenyi, Yongsheng Shi, Huaiguang Wu, Jinhua Liu, and Weiwei Zhang. "An adaptive enhancement algorithm based on visual saliency for low illumination images." *Applied Intelligence* 52, no. 2 (2022): 1770-1792. https://doi.org/10.1007/s10489-021-02466-4

[21] Zabani, Farah Nabilah, Haryati Jaafar, and Azian Harun. "Implementation of Fuzzy Gamma Adaptive Histogram Equalization for Penicillium and Aspergillus Species." In *Proceedings of the 11th International Conference on Robotics, Vision, Signal Processing and Power Applications: Enhancing Research and Innovation through the Fourth Industrial Revolution*, pp. 864-870. Singapore: Springer Singapore, 2022. https://doi.org/10.1007/978-981-16-8129-5_132

[22] Cardone, Barbara, Ferdinando Di Martino, and Sabrina Senatore. "A fuzzy partition-based method to classify social messages assessing their emotional relevance." *Information Sciences* 594 (2022): 60-75. https://doi.org/10.1016/j.ins.2022.02.028

[23] Sánchez, José Salvador, Filiberto Pla, and Francesc J. Ferri. "On the use of neighbourhood-based non-parametric classifiers." *Pattern Recognition Letters* 18, no. 11-13 (1997): 1179-1186. https://doi.org/10.1016/S0167-8655(97)00112-8